A Study on Autocascade Refrigeration System Using Carbon Dioxide and R134a Mixture

Soo-Nam Park* and Min-Soo Kim**

Key words : Alternative refrigerant, Carbon dioxide, Separator, Evaporative condenser, Mass fraction, Autocascade system

Abstract

Investigation of the performance of an autocascade refrigeration system using the refrigerant mixtures of R744 (carbon dioxide) and R134a (1,1,1,2-tetrafluoroethane) has been carried out by simulation and experiment. Cycle simulation using a constant UA model in heat exchangers has been performed for R744/134a mixtures of the compositions ranging from 10/90 to 30/70 by weight. Variations of mass flow rate of refrigerant, compressor work, refrigeration capacity and COP with respect to mass fraction of R744/134a mixture were presented. Performance test has been executed in the autocascade refrigeration system by varying secondary fluid temperatures at evaporator and condenser inlets. Experimental results match quite well with those obtained from the simulation.

Nomenclature

A : Heat transfer area [㎡]
COP : Coefficient of performance
C_p : Specific heat [kJ/kgK]
D : Tube diameter [m]
h : Enthalpy [kJ/kg] or heat transfer coefficient [W/㎡K]
h_{fg} : Latent heat of vaporization [kJ/kg]
m : Clearance volume ratio
$\dot{m}$: Mass flow rate [kg/s]
P : Pressure [kPa]
Q_v : Volumetric cooling capacity [kJ/㎥]
$\dot{Q}_c$: Heating capacity [kW]
$\dot{Q}_e$: Refrigeration capacity [kW]
T : Temperature [°C]
ΔT_{LMTD} : Log mean temperature difference[°C]
T_w : Secondary fluid temperature [°C]
ΔT_w : Secondary fluid inlet and outlet temperature difference [°C]

* Institute of Advanced Machinery and Design, Seoul National University, Seoul 151-742, Korea
** School of Mechanical and Aerospace Engineering, Seoul National University, Seoul 151-742, Korea

U : Overall heat transfer coefficient [W/m²K]
$\dot{V}_{comp}$: Compressor displacement rate [m³/s]
v : Specific volume [m3/kg]
$\dot{W}$: Compressor power consumption [kW]
x : Quality
X : Liquid composition
Y : Vapor composition

Greek symbols

η_{isen} : Isentropic efficiency
η_v : Volumetric efficiency

Subscripts

b : Brine
c : Condenser
e : Evaporator
f : Saturated liquid
g : Saturated vapor
isen : Isentropic process
r : Refrigerant
sat : Saturation
sub : Subcooled
sup : Superheated
tp : Two-phase

1. Introduction

Environmental safety and energy utilization efficiency in thermal systems have drawn lots of attention. Refrigerants used in refrigerators, air conditioners and heat pumps are one of the key factors in this discussion[1]-[5]. As CFC (chlorofluorocarbon) refrigerants were known to influence ozone layer depletion and global warming, they have been almost phased out in accordance with international agreements. In addition to this, the use of HCFC (hydrochlorofluorocarbon) refrigerants are being regulated in the future. Therefore, many researches are trying to find or develop new environmentally acceptable refrigerants. Even though HFC (hydrofluorocarbon) refrigerants have no influence on the ozone layer depletion, they are believed to have some effects on the global warming, which represents it is not best alternative refrigerant. It must be a better solution to use naturally occurring and environmentally harmless substances as alternative refrigerants. Among these natural refrigerants, carbon dioxide (CO_2) is environmentally friendly, nonflammable, nontoxic, easily available, and has excellent thermophysical properties. However, it is a disadvantage that the operating pressure of the refrigeration system using pure carbon dioxide is too high. One method to overcome this can be a choice of autocascade refrigeration system where CO_2 is used as a main working fluid and other refrigerant with lower vapor pressure is used to cool main working fluid. By doing so, the operating pressure can be reduced.

So far, a few papers on refrigeration systems using carbon dioxide have been published[6]-[10]. These studies have compared transcritical cycles using carbon dioxide with conventional vapor compression cycles using halocarbon refrigerants and showed that the adoption of carbon dioxide as working fluid reduces the size of the system and enhances a compression efficiency with low compression ratio. However, little work is carried out for an autocascade refrigeration system using CO_2.

This paper investigates the performance variations of an autocascade refrigeration cycle using carbon dioxide and R134a. Simulation and Experimental results will be pro-

vided for several mass fractions of R744 in the R744/134a mixtures and for different secondary fluid temperatures entering evaporator and condenser. The choice of HFC refrigerant, R134a as a component in the mixture is at our convenience. In order to make the working fluid purely natural, some other fluid such as hydrocarbon or other natural refrigerant should be considered.

2. Cylce simulation of autocascade refrigeration system

2.1 Operation principles

Schematic diagram of an autocascade refrigeration system is represented in Fig. 1, and the cycle is shown on the pressure- enthalpy diagram in Fig. 2. This autocascade refrigeration cycle consists of a compressor, a condenser, expansion valves, an evaporator and heat exchangers, and additional components such as a phase separator and an evaporative condenser (aftercondenser).

The refrigerant (point 2) which has been compressed to high temperature and pressure by compressor rejects heat to secondary fluid at condenser and becomes two phase fluid (point 3). In the phase separator, the refrigerant from the condenser is separated into a vapor where the composition of R744 is relatively high, and a liquid where the composition of R134a is relatively high. The liquid refrigerant (point 4) from the separator undergoes a pressure drop through an expansion valve and becomes a low temperature fluid (point 5) by an isenthalpic expansion process. It evaporates to saturated vapor (point6) by absorbing heat from the vapor refrigerant coming from the phase separator (point 8), which is condensed into saturated

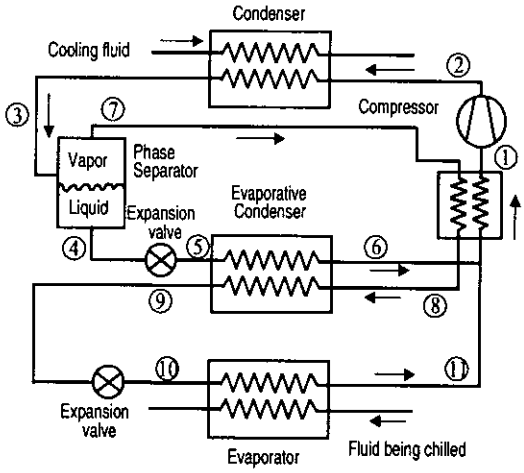

Fig. 1 Schematic diagram of an autocascade refrigeration system[11].

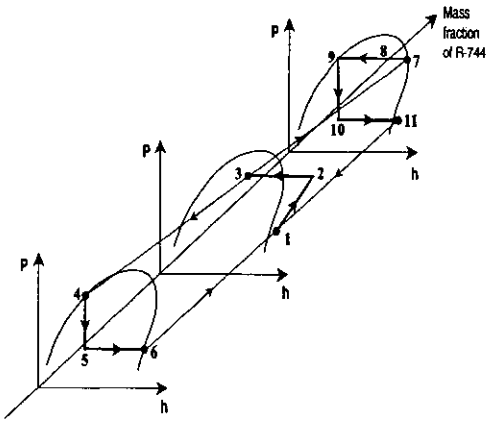

Fig. 2 Pressure-enthalpy diagram of an autocascade refrigeration system.

liquid (point 9) in the evaporative condenser. The condensed refrigerant of CO_2-rich mixture is expanded to be a low pressure and low temperature fluid (point 10). It becomes a superheated vapor (point 11) by a heat exchange with secondary fluid at evaporator and is mixed with R134a-rich refrigerant (point 6) coming from evaporative condenser. The temperature of the mixed refrigerant rises (point 1) through a heat exchange with the vapor

refrigerant coming from the separator. The compressor receives the low pressure refrigerant from the heat exchanger, and it forms a complete cycle

2.2 Component modeling

2.2.1 Compressor

Compression process is modeled to have a constant isentropic efficiency of 0.8. Enthalpy of refrigerant after compression and the compressor work is expressed as in Eqs. (1) and (2).

$$h_2 = h_1 + \frac{h_{2,isen} - h_1}{\eta_{isen}} \tag{1}$$

$$\dot{W} = \dot{m}_r(h_2 - h_1) \tag{2}$$

Subscripts 1 and 2 represent inlet and outlet, respectively. Compressor displacement rate is assumed constant. The mass flow rate of refrigerant is calculated considering the following volumetric efficiency[12].

$$\eta_v = 1 - m\left(\frac{v_1}{v_{2,isen}} - 1\right) \tag{3}$$

$$\dot{m}_r = \frac{\dot{V}_{comp}\eta_v}{v_1} \tag{4}$$

Here, m is a clearance volume ratio to have a constant value of 0.04. From compressor work and volumetric flow rate, COP and Q_v are expressed as in Eqs. (5) and (6).

$$COP = \frac{\dot{Q}_e}{\dot{W}} \tag{5}$$

$$Q_v = \frac{\dot{Q}_e}{\dot{V}_{comp}} \tag{6}$$

2.2.2 Condenser and Evaporator

During condensation process, the refrigerant undergoes desuperheating, two phase condensation, and subcooling. Also in the evaporation process, the refrigerant experiences two phase evaporation and superheating. Therefore, condenser and evaporator can be divided into several regions. Mean temperature difference of condenser and evaporator with counterflow is shown in Eqs. (7) and (8) with an assumption of constant UA for each heat exchanger[13].

$$\frac{1}{\Delta T_c} = \frac{\dot{Q}_{sup,c}}{\dot{Q}_c \Delta T_{sup,c}} + \frac{\dot{Q}_{tp,c}}{\dot{Q}_c \Delta T_{tp,c}} \tag{7}$$

$$\frac{1}{\Delta T_e} = \frac{\dot{Q}_{tp,e}}{\dot{Q}_e \Delta T_{tp,e}} + \frac{\dot{Q}_{sup,e}}{\dot{Q}_e \Delta T_{sup,e}} \tag{8}$$

Transferred heat from the condenser and to the evaporator is calculated by using mean temperature difference, which are expressed as in Eqs. (9) and (10).

$$\dot{Q}_e = (UA)_e \Delta T_e \tag{9}$$

$$\dot{Q}_c = (UA)_c \Delta T_c \tag{10}$$

2.2.3 Expansion device

Expansion device has functions of controlling mass flow rate of refrigerant and decreasing the pressure of refrigerant. Expansion device is modeled to be isenthalpic.

2.2.4 Evaporative condenser

Evaporative condenser is used to condense high pressure refrigerant using latent heat of vaporization of relatively low pressure refrigerant. Evaporative condenser is idealized to have an effectiveness of one.

2.3 Simulation conditions

In the autocascade refrigeration system, e-

vaporating temperature, condensing temperature, dryness at condenser outlet, the ratio of mass flow rate at the branch circuit, and the mass fraction of the refrigerant are important variables. In order to investigate the effects of the variation of these variables on the system performance, secondary fluid temperature at condenser and evaporator, degree of superheat and isentropic efficiency are assumed to be constant. Condensing pressure is defined as mean value between dew point pressure and bubble point pressure at condenser outlet temperature. Temperatures and compositions are selected to avoid the difficulty caused by the low critical temperature of R744 in calculating thermodynamic properties near the critical point using REFPROP[14]. Dependence of the performance on the variation of the secondary fluid temperature at evaporator inlet and the mass fraction of R744 is investigated under aforementioned simulation conditions. Simulation conditions in this study is shown in Table 1.

2.4 Simulation results

When the mass fraction of R744 whose specific volume is smaller than that of R134a increases or secondary fluid temperature at evaporator inlet increases, the specific volume of the refrigerant mixture entering the compressor decreases, which results in an increase of the mass flow rate as shown in Fig. 3. The power required by the compressor is calculated as the product of mass flow rate and enthalpy change during compression. Any increase of mass fraction of R744 requires more compression work since the saturation pressure of R744 is much higher than that of R134a, and therefore power consumption increases as shown in Fig. 4.

Table 1 Simulation conditions of autocascade refrigeration cycle using R744/134a mixtures

Variables	Value
Mass fraction of R744 in R744/134a mixture (wt%)	10, 15, 20, 25, 30, 35
UA of condenser (kW/℃)	0.3
UA of evaporator (kW/℃)	0.2
Secondary fluid temperature at evaporator inlet (℃)	-10, -5, 0, 5, 10
Secondary fluid temperature at condenser inlet (℃)	20, 25, 30
Temperature difference of secondary fluid between inlet and outlet at condenser (℃)	10.0
Temperature difference of secondary fluid between inlet and outlet at evaporator (℃)	8.0
Degree of superheat (℃)	5.0
Effectiveness of heat exchanger	1.0
Isentropic efficiency of compressor	0.8

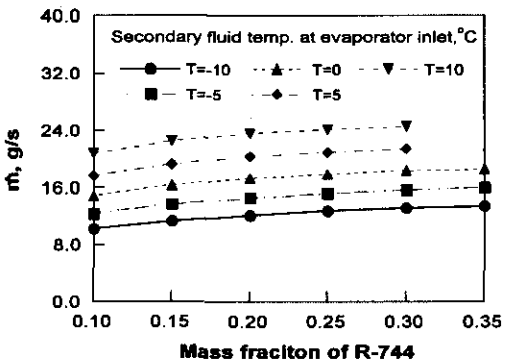

Fig. 3 Variations of mass flow rate of refrigerant with respect to mass fraction of R744 ($T_{w,c,in}$ = 20℃, $T_{w,c,out}$ = 30℃, $\Delta T_{w,e}$ = 8℃).

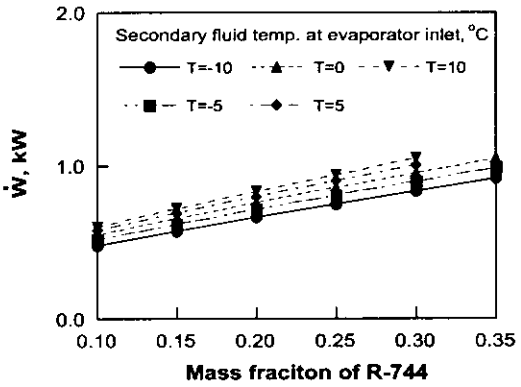

Fig. 4 Variations of compressor work with respect to mass fraction of R744 ($T_{w,c,in}$ = 20℃, $T_{w,c,out}$ = 30℃, $\Delta T_{w,e}$ = 8℃).

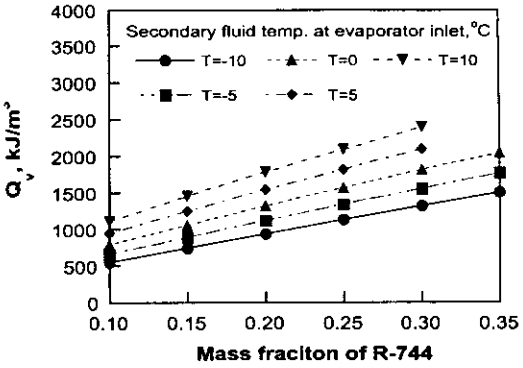

Fig. 5 Variations of volumetric cooling capacity with respect to mass fraction of R744 ($T_{w,c,in}$ = 20℃, $T_{w,c,out}$ = 30℃, $\Delta T_{w,e}$ = 8℃).

As the mass fraction of R744 increases, the refrigeration capacity which is the product of refrigerating effect and mass flow rate increases due to the increase of mass flow rate and higher latent heat of R744 than that of R134a during evaporation. Also, the refrigeration capacity increases with the elevation of secondary fluid temperature at evaporator inlet due to an increase of the mass flow rate. Fig. 5 shows the effects of the mass fraction of R744 and the secondary fluid temperature at evaporator inlet on volumetric cooling capacity when secondary fluid temperature entering condenser is 20℃ and Fig. 6 shows the COP. The volumetric cooling capacity is the refrigeration capacity divided by specific volume of the suction vapor entering the compressor. As the mass fraction of R744 or the secondary fluid temperature at evaporator inlet increases, the refrigeration capacity increases and the specific volume of R744/134a mixture decrease. Therefore, the volumetric cooling capacity increases with these variations. The COP is the refrigeration capacity divided by the power required by compressor. As shown in Fig. 6, when the mass fraction of R744 or the secondary fluid temperature at evaporator inlet increases, the increasing rate of the refrigeration capacity precedes that of required compressor power and thus COP increases. In general, it is known that the volumetric cooling capacity increases and the COP decreases as the composition with higher saturation pressure increases. But in this autocascade refrigeration cycle, both of the

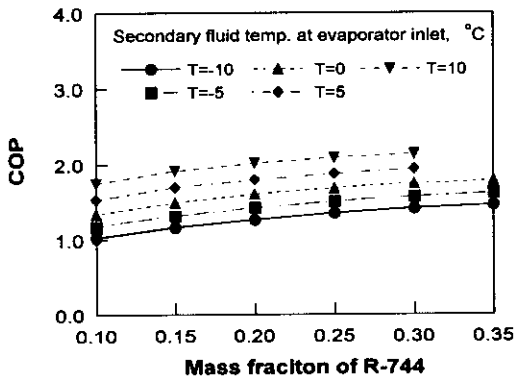

Fig. 6 Variations of COP with respect to mass fraction of R744 ($T_{w,c,in}$ = 20℃, $T_{w,c,out}$ = 30℃, $\Delta T_{w,e}$ = 8℃).

volumetric cooling capacity and COP increase. This is explained as below. As the mass fraction of R744 increases, dryness at condenser outlet also elevates, so the mass flow rate of CO_2 rich line from the phase separator increases. Because the increase rate of mass flow rate in CO_2 rich line from the phase separator is larger than that of total mass flow rate as the mass fraction of R744 increases, the increasing rate of refrigeration capacity precedes that of required compressor power and thus COP increases.

3. Performance experiment

3.1 Experimental setup

Experimental setup consists of a compressor, a condenser, two expansion valves, an evaporator, an evaporative condenser, and a phase separator as shown in Fig. 7. The compressor, which has two cylinders, is hermetically sealed reciprocating type. The diameter of the cylinder is 39.7 mm and the stroke is 23.8 mm. The condenser and the evaporator are manufactured as counterflow type heat exchangers with dual concentric tubes where the refrigerant flows inside the inner tube and the secondary fluid flows through the annulus. Inner tube has inner diameter of 7.5 mm and outer diameter of 9.5 mm and those for outer tube are 13.9 mm and 15.9 mm. The length of the tubes is 10 m in the evaporator and 15 m in the condenser. Metering valves, which can regulate the flow rate, were used as expansion valves. A plate-type heat exchanger was installed as an evaporative condenser. The temperatures at inlet and outlet of condenser and evaporator were measured with T-type thermocouples which were directly inserted

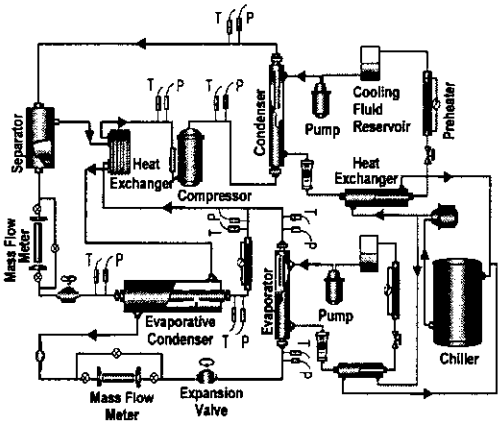

Fig. 7 Schematic diagram of experimental setup for autocascade refrigeration system using carbon dioxide and R134a.

into the tubes. The pressure was measured with absolute pressure transducers with an accuracy of ±0.2%. The secondary fluid temperature was kept constant by a PID temperature controller. The mass flow rate was measured by mass flow meters with an accuracy of about ±0.5%. The power required by the compressor was measured with a power meter.

3.2 Test conditions

The performance test was carried out for the refrigerant mixtures of R744/134a (24/76, 36/64 wt%) with secondary fluid temperatures of 25℃ and 35℃ at condenser inlet, and those of 0℃, 5℃, and 10℃ at evaporator inlet. Temperature difference of secondary fluid between inlet and outlet at condenser is controlled to be 10℃ and that at evaporator is adjusted to 8℃. When the variations of temperatures, pressure and mass flow rate were within ± 0.3℃, ±5 kPa, and ±0.2 g/s, respectively, the system was assumed steady and data were collected. The refrigerant mixture was pre-

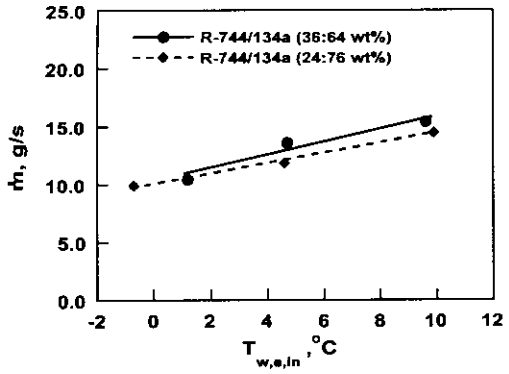

Fig. 8 Variations of mass flow rate of refrigerant with respect to secondary fluid temperature at evaporator inlet ($T_{w,c,in}$ = 25℃, $T_{w,c,out}$ = 35℃, $\Delta T_{w,e}$ = 8℃).

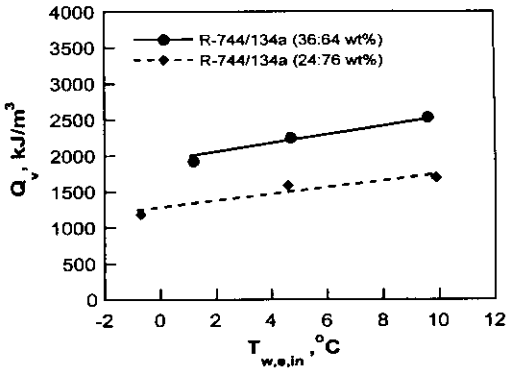

Fig. 10 Variations of volumetric cooling capacity with respect to secondary fluid temperature at evaporator inlet ($T_{w,c,in}$ = 25℃, $T_{w,c,out}$ = 35℃, $\Delta T_{w,e}$ = 8℃).

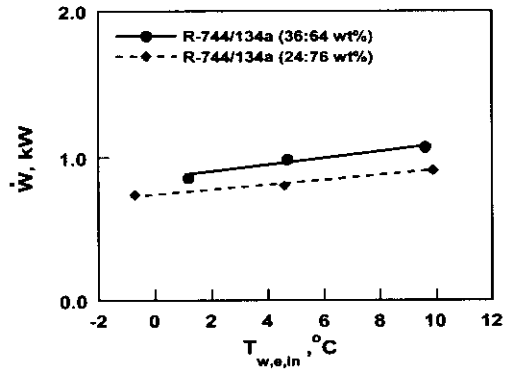

Fig. 9 Variations of compressor work with respect to secondary fluid temperature at evaporator inlet ($T_{w,c,in}$ = 25℃, $T_{w,c,out}$ = 35℃, $\Delta T_{w,e}$ = 8℃).

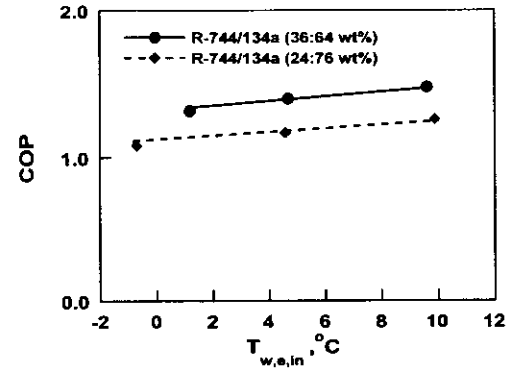

Fig. 11 Variations of COP with respect to secondary fluid temperature at evaporator inlet ($T_{w,c,in}$ = 25℃, $T_{w,c,out}$ = 35℃, $\Delta T_{w,e}$ = 8℃).

pared before the test and the mixture was injected to the evacuated system as liquid phase. The composition of circulating refrigerant mixtures was checked with gas chromatograph, and the accuracy is within ±0.005 of mole fraction.

3.3 Test results

The mass flow rate and the compressor power consumption are shown in Figs. 8 and 9, respectively. The mass flow rate gradually increases as the secondary fluid temperature at the evaporator inlet increases. This is due to the decreased specific volume at the compressor inlet, as the mean evaporating temperature is elevated. As stated in theprevious section, when the composition of R744/134a mixture increases, the mass flow rate in-

creases. This is mainly due to the smaller specific volume of R744 than that of

R134a for the same temperature and pressure condition, when displacement rate of compressor is kept constant. Compressor power consumption is increasing when the fraction of R744 increases, which is due to the increased mass flow rate and the higher inlet pressure of refrigerant mixture. The variation of volumetric capacity and COP with the change of the mass fraction of R744 and the secondary fluid temperature at evaporator inlet are represented in Figs. 10 and 11, respectively. The volumetric cooling capacity and COP increase, as the temperature of secondary heat transfer fluid at evaporator inlet is elevated and the fraction of R744 in the mixture increases. It is noteworthy that the variation in COP is not so sensitive to the change in secondary fluid temperature, which represents the mass flow rate of CO_2 -rich line from the phase separator is also increased due to the increased dryness when the fraction of R744 increases.

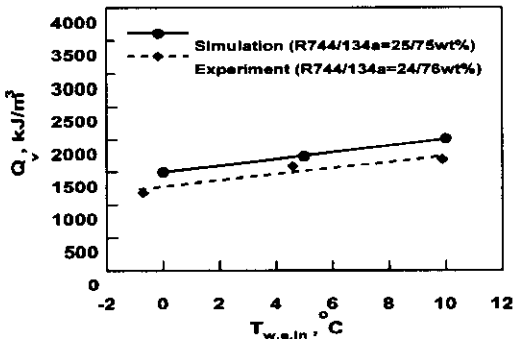

Fig. 12 Comparison of volumetric cooling capacity of experimental results and simulation results for autocascade refrigeration system with respect to secondary fluid temperature at evaporator inlet ($T_{w,c,in}$ = 25℃, $T_{w,c,out}$ = 35℃, $\Delta T_{w,e}$ = 8℃).

4. Comparison of simulation and experimental results

When mass fraction of R744/134a is 25/75 wt% for simulation and 24/76 wt% for experiment, comparisons of simulation and experimental results have been carried out where secondary fluid temperature at evaporator inlet is kept from 0℃ to 10℃ and that at condenser inlet is kept at 25℃ or 35℃. Temperature difference of secondary fluid between inlet and outlet at condenser is controlled to be 10℃ and that at evaporator is adjusted to 8℃.

The volumetric cooling capacity with respect to variations of secondary fluid temperature at evaporator is expressed in Fig. 12. The values measured in the experiment shows lower values than those in the simulation. This is partly due to pressure drop in the evaporator. Pressure drop in evaporator induces high specific volume in compressor and low mass flow rate of refrigerant, therefore cooling ca-

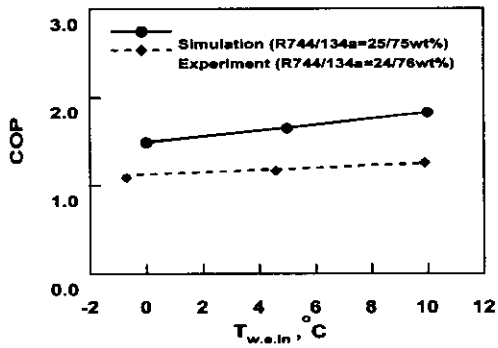

Fig. 13 Comparison of COP of experimental results and simulation results for autocascade refrigeration system with respect to secondary fluid temperature at evaporator inlet ($T_{w,c,in}$ = 25℃, $T_{w,c,out}$ = 35℃, $\Delta T_{w,e}$ = 8℃).

pacity and volumetric cooling capacity are reduced. Figure 13 shows COP where values measured in the experiment are lower than those in the simulation. Experimental results show similar tendencies with the results of simulation. Volumetric cooling capacity and the COP from the experiment are smaller in the experiment than those in the simulation where pressure drop in the evaporator and other irreversible losses in the compressor including friction loss were not considered.

5. Conclusions

Performance of autocascade refrigeration cycle using carbon dioxide and R134a has been investigated. Cycle simulation using constant UA model for evaporator and condenser has been performed. Variations of mass flow rate of refrigerant, compressor work, refrigeration capacity, volumetric cooling capacity and coefficient of performance (COP) with respect to mass fraction of R744 in R744/134a mixture were investigated. The volumetric cooling capacity and COP increase as the secondary fluid temperature at the evaporator inlet and mass fraction of R744 increase.

Experiment has been carried out for R744 /134a (24/76 and 36/64 wt%), where secondary fluid temperature at evaporator inlet is kept from 0℃ to 10℃ and that at condenser inlet is kept at 25℃ or 35℃. The volumetric cooling capacity and COP increase as the secondary fluid temperature at the evaporator inlet and mass fraction of R744 increase but the rate of increase of COP became smaller. Experimental results for autocascade refrigeration cycle were compared with simulation results. The variations of volumetric cooling capacity and COP showed similar trend for both cases.

Acknowledgements

This work has been supported by the Korea Research Foundation made in the program year of 1998. The support from the BK-21 Project of the Ministry of Education is greatly appreciated.

References

(1) Cavallini, A., 1995, Working fluids for mechanical refrigeration, *Proceedings of the 19th International Congress of Refrigeration*, The Hague, The Netherlands, Vol. IVa, pp. 25-42.

(2) Chang, Y. S., Kim, M. S. and Ro, S. T., 1997, Performance and heat transfer of an air conditioning system filled with hydrocarbon refrigerants, *Trans. of the Korean Society of Mechanical Engineers* (B), Vol. 21, No. 5, pp. 713-723.

(3) Didion, D. A. and Bivens, D. B., 1990, Role of refrigerant mixtures as alternatives to CFCs, *Int. J. Refrig.*, Vol. 13, pp. 163-175.

(4) Greenpeace, 1994, Hydrocarbons-High-Tech in Refrigeration, Hamburg, Germany.

(5) Kruse, H., 1996, Current status of natural working fluids on refrigeration, A/C, and Heat Pump Systems, *IIR Commissions B1, B2, E1 & E2, Applications for Natural Refrigerants*, Aarhus, Denmark, Sep. 3-6, pp. 49-64.

(6) Lorentzen, G. and Pettersen, J., 1993, A new, efficient and environmentally benign system for car air-conditioning, *Int. J. Refrig.*, Vol. 16, pp. 4-12.

(7) Lorentzen, G., 1993, Application of natural refrigerants, *IIR Commission B1 &*

B2, Ghent, Belgium, pp. 55-64.

(8) Lorentzen, G., 1994, Revival of carbon dioxide as a refrigerant, *Int. J. Refrig.*, Vol. 17, No. 5, pp. 292-301.

(9) Pettersen, J., 1994, An efficient new automobile air-conditioning system based on CO_2 vapor compression, *ASHRAE Trans.*, Symposia, pp. 657-665.

(10) Pettersen, J., 1995, Refrigeration, air conditioning and heat pump systems based on CO_2, Workshop Proceedings-Compression Systems with Natural Working Fluids, Trondheim, Norway, pp. 163-180.

(11) Stoecker, W. F., Industrial Refrigeration, Business News Publishing Company, Vol. II, pp. 319-325.

(12) Stoecker, W. F., Jones, J. W., 1982, Refrigeration & Air conditioning, 2nd ed., McGraw-hill Book Company.

(13) Domanski, P. A., McLinden, M. O., 1992, A simplified cycle simulation model for the performance rating of refrigerants and refrigerant mixtures, *Int. J. Refrig.*, Vol. 15, No. 2, pp. 81-88.

(14) Huber, M., Gallagher, J., McLinden, M. and Morrison, G., Thermodynamic properties of refrigerants and refrigerant mixtures, Ver. 5.0, NIST, Gaithersburg, U.S.A.

(15) Park, S. N. and Kim, M. S., 1999, Performance of autocascade refrigeration system using carbon dioxide and R134a, *Korean Journal of Air Conditioning and Refrigeration Engineering*, Vol. 11, No. 6, pp. 880-890.

(16) Park, S. N. and Kim, M. S., 1997, Performance analysis of refrigeration cycle using carbon dioxide and R134a, *Proceedings of the Society of Air Conditioning and Refrigeration Engineers of Korea '97 Annual Summer Conference*, Korea, Vol. 2, pp. 92-96.